INTERNATIONAL TRANSACTIONS ON ELECTRICAL ENERGY SYSTEMS
Int. Trans. Electr. Energ. Syst. 2016; **26**:884–900
Published online 28 July 2015 in Wiley Online Library (wileyonlinelibrary.com). DOI: 10.1002/etep.2114

Extracting the transient events from power system signals by independent component analysis

Danton D. Ferreira[1]*,†, José M. de Seixas[2], Augusto S. Cerqueira[3], Carlos A. Duque[3], Math H. J. Bollen[4] and Paulo F. Ribeiro[5]

[1] *Engineering Department, Federal University of Lavras, Lavras, Minas Gerais, Brazil*
[2] *Federal University of Rio de Janeiro, COPPE/Poli, Rio de Janeiro, RJ, Brazil*
[3] *Department of Electrical Circuits, Federal University of Juiz de Fora, Campus Universitário, Juiz de Fora, MG, Brazil*
[4] *Department of Engineering Sciences and Mathematics, Energy Science Division, Luleå University of Technology, Luleå, Sweden*
[5] *Department of Electrical Engineering, Federal University of Itajubá, Itajubá, MG, Brazil*

SUMMARY

This paper presents a method for extracting transient events from the power system signal based on independent component analysis. The extraction of transients is important to diagnose the system in terms of power quality, because the computation of power quality indices from the extracted events is more efficient and easier to be carried out. Furthermore, the proposed method can be applied as a preprocessing tool for transient characterization in disturbance detection, classification, and identification systems. Both qualitative and quantitative analyses demonstrate the efficiency and the advantages of the proposed method in comparison with other approaches commonly used for the same purpose. Copyright © 2015 John Wiley & Sons, Ltd.

KEY WORDS: independent component analysis; transients; electric power quality

1. INTRODUCTION

The increased use of power electronics applications, which include renewable energy generation, nonlinear loads, drives, and so on, have contributed to the degradation of power quality (PQ). As a consequence, transients, harmonics, voltage variations can reach levels that interfere with the performance of other loads and system equipment. Also, with the decentralized energy generation, the PQ has become one of the most important subjects to select the best utility.

An important class of disturbance is the transient, which is defined, in power systems analysis, as short-duration deviations from steady-state voltage or current waveforms [1]. These PQ transients are broadly defined by the IEEE 1159–2009 standard [2]. The main causes of transients are lightning strokes, self-clearing faults, and switching actions like capacitor switching. The correct characterization of transients is an important requirement in order to find their causes and to take corrective actions. Transients can be characterized from their magnitude, spectral component, and time duration values, but other features may be extracted for providing additional information. Based on this definition, a wide variety of transients may appear in the power system, making the process of estimation and quantification of PQ a difficult task [3].

Therefore, according to the international standard International Electrotechnical Commission 61000-4-30 [4], the detection, classification, and characterization of transient voltages are challenging subjects. Some of the transient detection methods and examples of application include the following [4]: (i) *comparative method*: when a fixed, absolute threshold is exceeded, a transient is detected,

*Correspondence to: Danton D. Ferreira, Engineering Department, Federal University of Lavras, Lavras, Minas Gerais, Brazil.
†E-mail: danton@deg.ufla.br

Copyright © 2015 John Wiley & Sons, Ltd.

for example, surge protective devices (SPDs) that are sensitive to the total voltage; (ii) *envelope method*: similar to comparative method, but with the fundamental removed prior to analysis, for example, for instances of capacitive coupled transients; (iii) *sliding-window method*: the instantaneous values are compared with the corresponding values on the previous cycle, for example, low-frequency switching transients associated with capacitor banks used for factor correction; (iv) *dv/dt method*: when a fixed, absolute threshold of *dv/dt* is exceeded, for example, mistrigger of power electronics circuits or nonlinear distribution on inductor winding; (v) *root mean square value* (*rms*) *value*: using very rapid sampling, the rms value is computed for intervals much less than one fundamental period and compared with a threshold, for example, when further computations are desirable such as energy deposition in an SPD or charge transfer; and (vi) other methods include frequency versus amplitude measurements (discrete or fast Fourier transform, wavelet, etc.).

Sophisticated methods have recently used transient extraction techniques for the correct estimation and quantification of PQ [3,5], as well as to support PQ disturbance detection and classification methods as an important preprocessing tool [6–8]. In [3] and [5], the transient waveform is estimated by subtracting an estimate of the fundamental waveform from the original waveform. In order to estimate the fundamental waveform, Naik and Kundu [3] and Shin *et al*. [5] used time-frequency distribution for amplitude evaluation and a curve-fitting routine to obtain the phase, and from this, extracting PQ indices. Differently, Liu *et al*. [6] used the DB4 wavelet transform to extract the high frequency of transients aiming at classifying them. A high-pass filter (HPF) is applied in [8] to remove the lower frequencies from the voltage signal, and the resulting signal is used to distinguish between transients and waveform distortions. In [7], a second-order notch filter (NF) block (tuned to 60 Hz) is applied to estimate the transients in a voltage signal, in which the aim is to classify multiple disturbances.

When the monitored transient is due to capacitor switching, the efficient extraction of the transient content may also be useful for parallel resonant frequency estimation [9,10], as well as for determining the relative location of switched capacitor banks [11–13], because these actions are performed through the correct feature estimation of capacitor-switching transients.

A suitable way of detecting, classifying, and characterizing transients is to extract them before, that is, to isolate the transient component of the monitored signal. With this aim, Bollen and Gu [1] have discussed four commonly used methods: the cycle-by-cycle difference (CCD), comparison with average fundamental waveform (AFW), HPF, and NF. These methods are based on classical filtering and work very well in the case of stationary signals and in the case when the spectrum of the transient is disjoint from the spectrum of the normal signal. These two hypotheses can fail in several situations, for example, if the fundamental frequency changes in time the CCD method will generate false trigger. HPF and NF will not be able to separate the spectrum of the transient from the spectrum of the signal distorted by harmonic and so on. To overcome this situation, alternative methods must be used, among them, method based on statistical signal processing such as the independent component analysis (ICA) proposed in this paper.

Regarding ICA applications for PQ analysis, authors in [14], [15], and [16] developed ICA-based methods to estimate harmonic components from voltage signals in which promising results have been reported. ICA is a statistical signal-processing technique that separates a multivariate signal into additive independent component sources. Reference [17] proposed a method to identify and classify PQ disturbances based on ICA and support vector machine. In previous works [18,19], the authors exploited the ICA decomposition capability to develop a method for multiple and single PQ disturbance classification.

In the present paper, a new method based on single channel independent component analysis (SCICA) [20] is proposed to separate the transient events from the power system signals (current or voltage). This separation process is referred to as ‘extraction of the transient’. The advantages of the method proposed in this paper are the low cost in the operational stage, because it may be viewed as a low-order finite-impulse-response (FIR) filter, and its good performance. Unlike in [18] and [19], the method proposed here focuses on transient extraction from power signals by using a simple ICA-based FIR filter structure. Therefore, the main contribution of this paper lies in providing a good estimation of PQ transients. A comparative study by considering different types of simulated time-varying voltage signals with transients is presented. The method is also tested in real signals and resulted from a motor-start experiment, experimental three-phase voltage signals showing end of interruption with difference in reclosing instants and mild transformer saturation, and experimental three-phase voltage signals because of capacitor energizing.

Copyright © 2015 John Wiley & Sons, Ltd.

DOI: 10.1002/etep

According to Bollen and Gu [1], the CCD and the NF are the two most appropriate methods, and the literature lacks standard documents that discuss methods to extract the transient. In this context, this paper can be a good contribution for the area, proposing a new method for transient extraction and showing a comparative study.

2. THEORETICAL BACKGROUND

This section presents the existing methods used for comparison: CCD, AFW, HPF, and NF. These methods were chosen because each one is suitable for extracting a specific type of transient.

2.1. Cycle-by-cycle difference

This method is very simple and, basically, compares one cycle of the electrical signal waveform with the waveform one cycle earlier in time [1]. Despite its simplicity, it is important to be careful, however, regarding its limitations: (i) The same transient can come back twice, because after the transient, there is again a difference with the previous cycle. (ii) The transient duration is limited to one cycle. Alternatively, the first cycle of the recording is used in this case. This latter method has been used in this paper. (iii) The length of one cycle is not always exactly equal to an integer number of samples. Thus, comparing the signal value with the value one cycle back in time requires interpolation between samples, and it will make the implementation of the method more complicated. (iv) A change in fundamental voltage associated with the transient and time-varying harmonics will cause error in the extracted transient.

2.2. Comparison with average fundamental waveform

This method compares the monitored waveform with the fundamental waveform, which can be generated by a phase-locked loop. This method is easier to implement as there is no need for interpolation.

Despite its implementation facility, the extracted transient can be corrupted by a change in fundamental and harmonic distortion. According to Bollen and Gu [1], as the harmonic distortion is rarely less than a few percent of the fundamental, this will introduce a significant error in the extracted transient, especially for less severe transients.

This method was applied in this paper for comparison using the enhanced phase-locked loop proposed in [21].

2.3. High-pass filter

Initially, this method sounds like easy to be implemented, but its performance depends to a large extent on the properties of the filter [1]. The aim of the filter is to remove the fundamental component, and the passband should include all the possible frequency components of the transient. The choice for the stop-band edge and passband edge is not trivial, as the frequencies of the transient components are rarely known beforehand. However, depending on the passband choice, the extracted transient can be corrupted by harmonics. In order to avoid it, in [1], it is suggested to combine this method with the CCD, so that the HPF removes the fundamental component and so does the CCD with the harmonics. On the other hand, this approach cannot remove from the extracted transient the harmonic distortion associated with it. In addition, the method is prone to phase or magnitude error introduced by the digital filter.

As in [1], a third-order type II Chebyshev filter with a stop-band edge at 60 Hz was used in this paper to build the HPF method. The filter was designed with passband edge at 300 Hz, passband ripple 0.1 dB, and stop-band attenuation of 40 dB.

2.4. Notch filter

This method preprocesses the monitored waveform by an NF [22] tuned to the frequency of the fundamental component ($f_0 = 60$ Hz). Due primarily to low computational cost and higher selectivity at

Copyright © 2015 John Wiley & Sons, Ltd.

DOI: 10.1002/etep

the frequency of interest, it is recommended to use a second-order Infinite Impulse Response filter structure, whose z-transform is given by

$$H_0(z) = \frac{1 + a_0 z^{-1} + z^{-2}}{1 + \rho_0 a_0 z^{-1} + \rho_0^2 z^{-2}} \tag{1}$$

in which $a_0 = -2cos\omega_0$ and ρ_0 are the notch factors, with $0 \ll \rho_0 < 1$.

Unfortunately, this filter does not remove harmonic distortion. Thus, the difference between the extracted and the original transient is almost exclusively due to the harmonic distortion and change in fundamental.

According to Bollen and Gu [1], the extracted transient is the most suitable characteristic versus time for voltage and current transients.

3. SINGLE CHANNEL ICA-BASED METHOD FOR TRANSIENT EXTRACTION

According to Davies and James [20], the SCICA approach can be considered an extreme case (one sensor) of under-determined ICA, and it is an instance of multi-dimensional ICA applied to vectors of delayed samples. In using such approach, it is first necessary to form a 'multi-channel' representation of the data. This can be carried out by generating a series of delayed vectors taken from the observed signal $x[n]$, given by

$$\mathbf{x}[n] = [x[n],\ x[n-1]\ ,\ \ldots,\ x[n-M+1]]^T \tag{2}$$

Thus, the basic formulation of the ICA may be recovered, such as $\mathbf{x}[n] = \mathbf{A}\mathbf{s}[n]$, where $\mathbf{s}[n] = [s_1[n], s_2[n]\ ,\ \ldots,\ s_M[n]]^T$ is the statistically mutually independent component vector at sample n and $\mathbf{A}$ is an $M \times M$ matrix, which is called the mixing matrix. Then, the ICA algorithms [23] estimate the original source signals using only the time-delayed versions of the observed signal: $\mathbf{y}[n] = \mathbf{W}\mathbf{x}[n]$.

Here, $\mathbf{y}[n] = [y_1[n], y_2[n]\ ,\ \ldots,\ y_M[n]]^T$ represents the estimation of the independent component vector $\mathbf{s}[n]$, and $\mathbf{W}$ is the estimated de-mixing matrix. Thus, the row vectors of $\mathbf{W}$ can be interpreted as de-mixing FIR filters.

It is important to stress that the usage of the multi-dimensional model presented in (2) implies that the sources can only be successfully identified and separated when they have disjoint spectral support, as proved in [20]. Then, when ICA is applied to delayed vectors formed from a mixture of band-limited sources, it will identify a multiple number of components with each source proportional to the source bandwidth. Therefore, taking into account that the high-frequency power system events have disjoint spectra with respect to the fundamental component and low-order waveform distortions, the SCICA can be applied to the monitored power system signal for extracting high-frequency events from the electrical signals. A known class of high-frequency events in PQ is the transients, and it is with respect to them that we are going to refer from this point.

3.1. Design of the proposed method

The proposed method can be summarized by the design of a linear FIR filter based on the SCICA algorithm, and it can be divided into four steps, which are described as follows and can be depicted from Figure 1:

(1) Generate the time-delay representation $\mathbf{x}[n]$ using a design dataset (initially with one time delay), according to (2), and present it to the ICA algorithm in order to obtain the estimated de-mixing matrix $\mathbf{W}$. In this paper, the second-order blind identification algorithm [24] is used for source vector estimation.
(2) Find the row of the de-mixing matrix $\{\mathbf{W}_{(i,:)}\}$ that provides the best estimation of the transients (the linear FIR filter). For that, some measure should be used to evaluate the similarities between the extracted and the original events. Considering that, in this step, the magnitude and

Copyright © 2015 John Wiley & Sons, Ltd.

DOI: 10.1002/etep

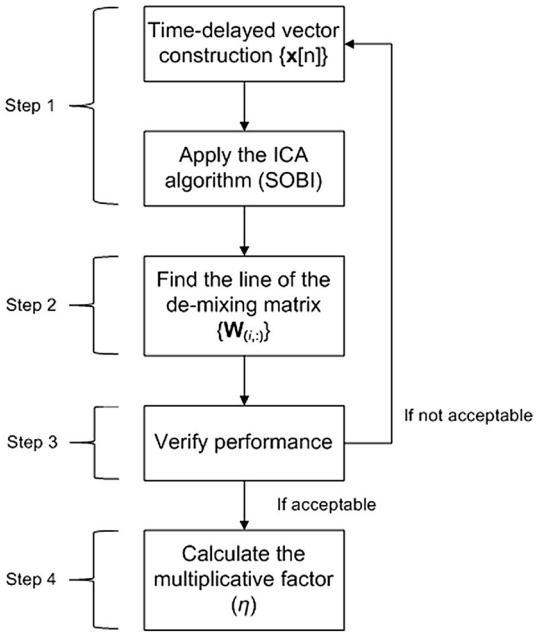


Figure 1. Chart flow of the design phase of the proposed method.

phase of the extracted transient were still not recovered; the linear correlation (*LC*) was used as similarity measure.

(3) Return to step 1 and increase the number of time delays until a desirable performance is achieved (the *LC* can be used).

(4) Finally, calculate the multiplicative factor η that recovers the magnitude and the phase of the extracted event, which can be achieved by a standard least square optimization technique [25].

It is worth to mention that these design steps must be performed using the training data, for which the original disturbance signal sources are known.

The operational stage of the proposed method consists of a vector multiplication:

$$\hat{e}[n] = \eta \mathbf{W}_{(i,:)} \mathbf{x}[n] \tag{3}$$

where $\hat{e}[n]$ is the extracted signal containing only the estimated high-frequency event information and $n = 1, \ldots, N$ is the sample index in an N-length frame. Thus, the computational cost of the proposed method may be given by $N(M-1)$ additions and NM multiplications, where N is the number of samples of the processed signal and M is the length of $\mathbf{W}_{(i,:)}$.

4. DATABASE

Simulations were carried out with several waveforms of the electrical signal with sampling rate equal to 15 360 Hz and the signal-to-noise ratio 60 dB. A set of 2500 high-frequency events (oscillatory and impulsive transients and notches) was randomly generated and equally divided into design dataset (used for system design) and test dataset (used in order to evaluate the system performance). Practical situations that can normally occur in a voltage signal have been included in the dataset, such that 500 events include fundamental component at frequency of 60 Hz, 500 fundamental frequency varying from 57 to 63 Hz (5% of variation), 500 changes in the amplitude of the fundamental component like sags, rapid voltage changes, and swells, 500 harmonics, and 500 variations in the amplitude of the harmonics.

According to Marques *et al.* [26], the power frequency normally varies very slowly over a small range. However, for weak power systems, the power frequency variation can be large;

Copyright © 2015 John Wiley & Sons, Ltd.

DOI: 10.1002/etep

for example, in [27], the frequency deviation can reach ±5% of its nominal value. Actually, this variation in fundamental frequency appears rather unrealistic, depending on the power system, but we have decided to simulate such situation aiming at evaluating the proposed method in a critical scenario.

In order to verify the efficiency of the proposed method for real signals, three cases of transients obtained experimentally are used.

5. RESULTS

This section presents the results of the proposed method in comparison with the existing methods discussed in Section 2 for both simulated and measured power system signals. It is divided into six cases, which represent the practical situations included in the simulated dataset and a specific synthetic test signal created by Bollen and Gu [1]. The values shown in Tables I–V are from averaging over 500 simulated events (average ± standard error).

5.1. From simulation

During system design, *LC* between the transient estimation and the original source was obtained (design database). Also, aiming at verifying the mixture residue in the estimated transient, an

Table I. Performance of the methods for voltage signals with transients.

Methods	*LC*	*Rr*	*Sd*
Proposed method ($M=3$)	0.85 ± 0.01	0.37 ± 0.01	0.02 ± 0.00
Proposed method ($M=5$)	0.94 ± 0.00	0.11 ± 0.01	0.01 ± 0.00
Cycle-by-cycle difference	1.00 ± 0.00	0.00 ± 0.00	0.00 ± 0.00
Comparison with average fundamental waveform	1.00 ± 0.00	0.00 ± 0.00	0.00 ± 0.00
High-pass filter	0.95 ± 0.01	0.09 ± 0.00	0.01 ± 0.00
Notch filter	1.00 ± 0.00	0.00 ± 0.00	0.00 ± 0.00

LC, linear correlation; *Rr*, residue ratio; *Sd*, spectral difference.

Table II. Performance of the methods for transient in a signal with fundamental frequency varying.

Methods	*LC*	*Rr*	*Sd*
Proposed method ($M=3$)	0.63 ± 0.03	0.63 ± 0.02	0.03 ± 0.00
Proposed method ($M=5$)	0.81 ± 0.02	0.47 ± 0.06	0.02 ± 0.00
Cycle-by-cycle difference	0.18 ± 0.02	151.10 ± 20.12	0.43 ± 0.03
Comparison with average fundamental waveform	0.25 ± 0.02	61.61 ± 7.92	0.28 ± 0.02
High-pass filter	0.68 ± 0.02	1.85 ± 0.28	0.04 ± 0.00
Notch filter	0.39 ± 0.03	15.49 ± 2.05	0.15 ± 0.01

LC, linear correlation; *Rr*, residue ratio; *Sd*, spectral difference.

Table III. Performance of the methods for voltage signals corrupted by transient and sag, swell, or rapid voltage change.

Methods	*LC*	*Rr*	*Sd*
Proposed method ($M=3$)	0.86 ± 0.01	0.36 ± 0.01	0.02 ± 0.00
Proposed method ($M=5$)	0.94 ± 0.00	0.11 ± 0.01	0.01 ± 0.00
Cycle-by-cycle difference	0.52 ± 0.04	14.93 ± 3.06	0.10 ± 0.01
Comparison with average fundamental waveform	0.59 ± 0.03	5.28 ± 0.86	0.07 ± 0.01
High-pass filter	0.94 ± 0.03	0.11 ± 0.01	0.01 ± 0.00
Notch filter	0.78 ± 0.02	1.24 ± 0.23	0.03 ± 0.00

LC, linear correlation; *Rr*, residue ratio; *Sd*, spectral difference.

Copyright © 2015 John Wiley & Sons, Ltd.

DOI: 10.1002/etep

Table IV. Performance of the methods for voltage signals corrupted by transient and harmonics.

Methods	*LC*	*Rr*	*Sd*
Proposed method ($M=3$)	0.86 ± 0.01	0.39 ± 0.05	0.02 ± 0.00
Proposed method ($M=5$)	0.93 ± 0.01	0.53 ± 0.14	0.02 ± 0.00
Cycle-by-cycle difference	1.00 ± 0.00	0.00 ± 0.00	0.00 ± 0.00
Comparison with average fundamental waveform	0.31 ± 0.01	13.07 ± 1.20	0.13 ± 0.00
High-pass filter	0.33 ± 0.01	10.65 ± 0.98	0.11 ± 0.00
Notch filter	0.30 ± 0.01	13.54 ± 1.19	0.13 ± 0.00

LC, linear correlation; *Rr*, residue ratio; *Sd*, spectral difference.

Table V. Performance of the methods for voltage signals corrupted by transient and time-varying harmonics.

Methods	*LC*	*Rr*	*Sd*
Proposed method ($M=3$)	0.85 ± 0.01	0.4 ± 0.05	0.02 ± 0.00
Proposed method ($M=5$)	0.93 ± 0.01	0.54 ± 0.12	0.02 ± 0.00
Cycle-by-cycle difference	0.78 ± 0.02	1.02 ± 0.22	0.03 ± 0.00
Comparison with average fundamental waveform	0.32 ± 0.01	12.98 ± 1.43	0.14 ± 0.00
High-pass filter	0.36 ± 0.01	9.66 ± 1.15	0.11 ± 0.00
Notch filter	0.33 ± 0.01	12.89 ± 1.57	0.13 ± 0.00

LC, linear correlation; *Rr*, residue ratio; *Sd*, spectral difference.

alternative index, here named as residue ratio (*Rr*), was computed from Equation (4), where $\hat{t}[n]$ and $t[n]$ are the extracted and the original transients, respectively.

$$Rr = \frac{\sum_{n=1}^{N} [t[n] - \hat{t}[n]]^2}{\sum_{n=1}^{N} t^2[n]} \tag{4}$$

Figure 2 shows the correlation (left) and *Rr* (right) indices for different time-delay representations ($M=2, 3, \ldots, 10$) (Equation (2)), revealing the two best performances are achieved when two and four time-delay versions were used (step 3). Thus, in the operational phase, a linear FIR filter with five coefficients will be used for the case with four time-delay versions. Once the filter order is established, the multiplicative factor η is found using a least square optimization technique (step 4).

Illustratively, Figure 3 shows the original transient in (a) and its spectrum in (b). This transient is part of an event randomly taken from the test set. Envisaging at comparing the performance of the proposed method when implemented by considering different numbers of time-delayed versions of the monitored signal, this event was processed by the proposed method considering one (worst case), three, and four time-delayed versions (best cases). It is possible to observe a residue from the first harmonic in the

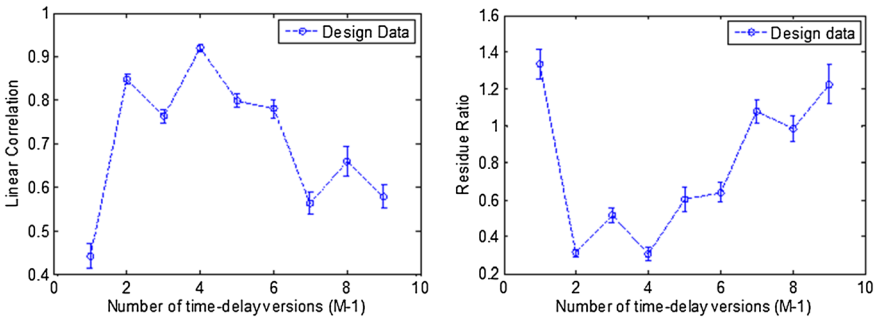


Figure 2. The average of the linear correlations between the original and the extracted transients (left) and the average of the *Rr* index (right).

Copyright © 2015 John Wiley & Sons, Ltd.

DOI: 10.1002/etep

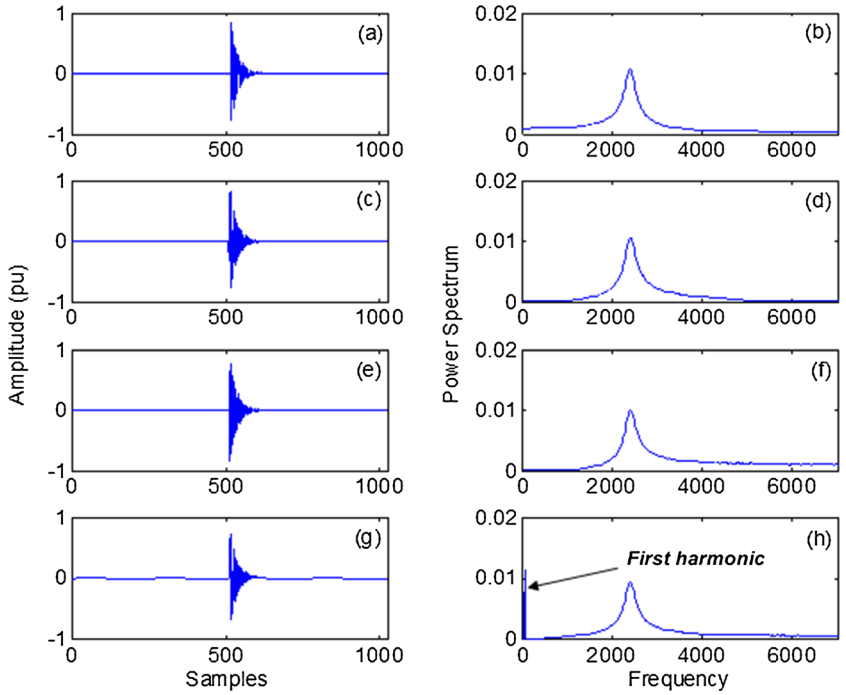


Figure 3. Original transient in (a) and its spectrum in (b); estimated transient in (c) and its spectrum in (d) considering four time-delay versions; estimated transient in (e) and its spectrum in (f) considering three time-delayed versions; and estimated transient in (g) and its spectrum in (h) considering one time-delay version.

transient estimated from one time-delayed version. For the best cases, the similarity between the estimated transient and the original one in both time and frequency domains can be noticed.

The proposed method was applied to the test dataset and compared with the four methods of transient extraction, as described in Section 2. The *LC* and *Rr* indices were applied to the extracted transients for performance evaluation in time domain. For performance evaluation in frequency domain, the spectral difference (*Sd*) between the extracted transient and the original one was calculated as

$$Sd_i = \sqrt{(S_i(f) - E_i(f))\cdot(S_i(f) - E_i(f))^T} \tag{5}$$

where $S_i(f)$ and $E_i(f)$ are the power spectra of the original transient and the extracted one, respectively. T superscript is the transposition operator.

5.1.1. Voltage signals with transients. Table I summarizes the quality of the extracted transients in terms of the *LC*, *Rr*, and *Sd* indices. One can see that all the methods, except the proposed method for $M=3$ (two time-delayed versions), have achieved good results, with *LC* higher than 0.90, *Rr* lower than 0.20, and *Sd* lower than 0.02. Figure 4 illustrates the distributions of the indices for each method. One can observe that the CCD, AFW, and NF methods produced the best results. Among the proposed methods, it is recommended the use of that with four time-delayed versions ($M=5$), for this case.

Figure 5 shows an example of the transient extracted from a given event from the test dataset. One can see that a good performance was achieved by all methods. A small residue from the fundamental component can be noted in the power spectrum of the transient extracted by the HPF method (pair (m)–(n)). The transient extracted by the proposed method (case $M=3$) was not shown for simplification.

5.1.2. Transient in a signal for which the fundamental frequency varies. The variation of the fundamental frequency was included by a change in value at the same instant the transient appears. Table II summarizes the quality of the extracted transients. One can see that the proposed method (case $M=5$)

Copyright © 2015 John Wiley & Sons, Ltd.

DOI: 10.1002/etep

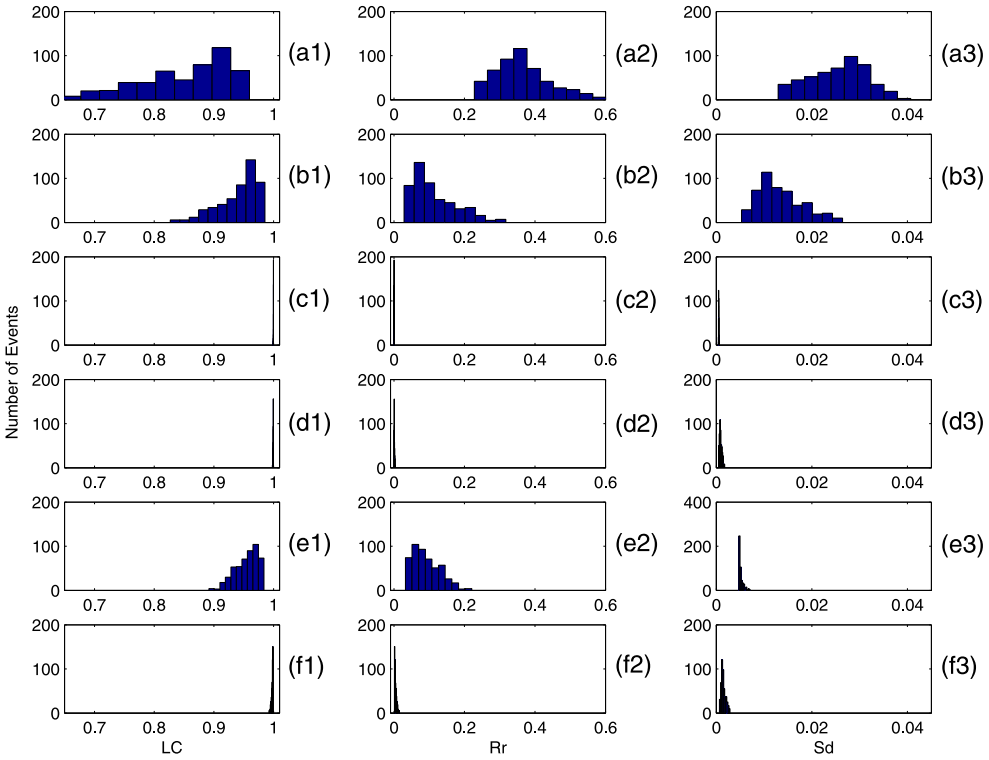


Figure 4. Distributions of the indices *LC*, *Rr*, and *Sd*, left for the methods for voltage signals with transients. The following threes from (a1)–(a2)–(a3) to (f1)–(f2)–(f3) show the *LC*, *Rr*, and *Sd* distributions as extracted from SCICA based ($M = 3$), SCICA based ($M = 5$), CCD, AFW, HPF, and NF methods, respectively.

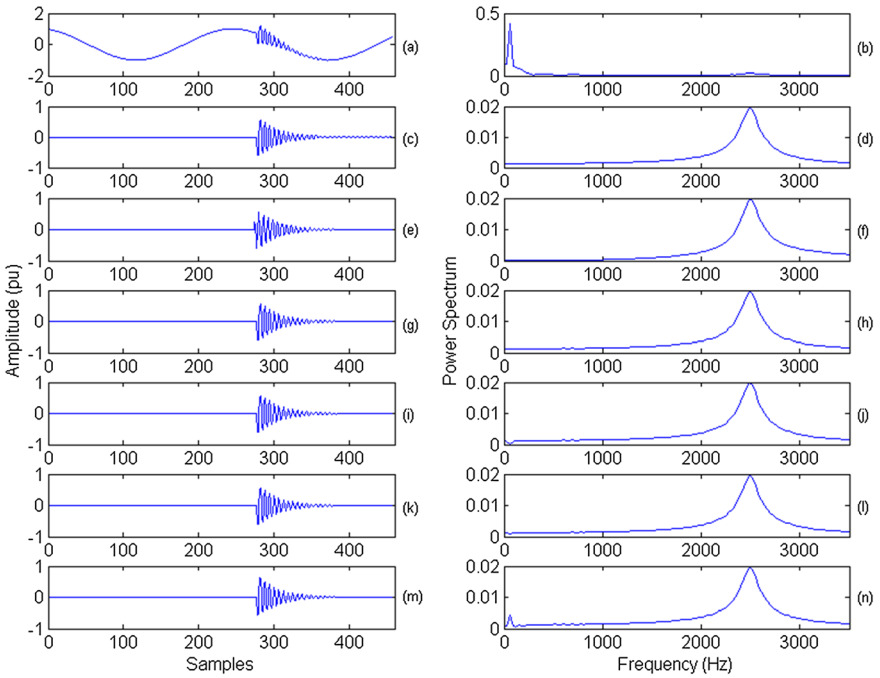


Figure 5. Voltage signal corrupted by oscillatory transient in (a) and its spectrum in (b). Original transient source in (c) and its spectrum in (d). The following pairs from (e)–(f) to (m)–(n) show the transient and its spectrum as extracted from SCICA based ($M = 5$), AFW, NF, CCD, and HPF methods, respectively.

Copyright © 2015 John Wiley & Sons, Ltd.

DOI: 10.1002/etep

was not as affected by the fundamental frequency variations as the other methods, keeping good results. The performance of the other methods reduced drastically with fundamental frequency variations. Among methods used for comparison, the CCD and AFW methods have collapsed.

Figure 6 illustrates the distributions of the indices for each method. One can observe that the proposed method (cases $M=5$ and $M=3$) and the HPF produced the best results.

Figure 7 shows an example of the transient extracted for a given event from the test dataset. One can clearly see that the methods AFW (pair (g)–(h)), NF (pair (i)–(j)), and CCD (pair (k)–(l)) are strongly affected by the fundamental frequency variations. The effect on HPF (pair (m)–(n)) method is not that huge in time domain, but it is better noticed in the spectrum.

5.1.3. Voltage signals corrupted by transient and sag, swell, or rapid voltage change. Here, low-frequency events (sag, swell, and rapid voltage change) have been added to the voltage signals corrupted by transient. High performance was achieved by the proposed method (case $M=5$) with $LC=0.94$, $Rr=0.11$, and $Sd=0.01$ (Table III). Among the other methods, the HPF achieved the higher performance, as it was expected, because this method is capable of removing the low-frequency events from the signal. Its performance was similar to the proposed method (case $M=5$).

5.1.4. Voltage signals corrupted by transient and harmonics. In order to verify the robustness of the methods to harmonics, we have included harmonics (until the seventh component) at the voltage signals corrupted by transient. The amplitudes (h_i) and phases (ϕ_i) of harmonics were randomly generated following a uniform distribution of values, in which $h_i \in [0, 0.2]$ per unit and $\phi_i \in [-\pi, +\pi]$. As in Table IV, the CCD method achieved extremely good performance ($LC=1.00$, $Rr=0.00$, and $Sd=0.00$), in this case. However, high performance was also achieved by the proposed method (case $M=5$), and, for $M=3$, it was not so bad. The other methods produced much worse results.

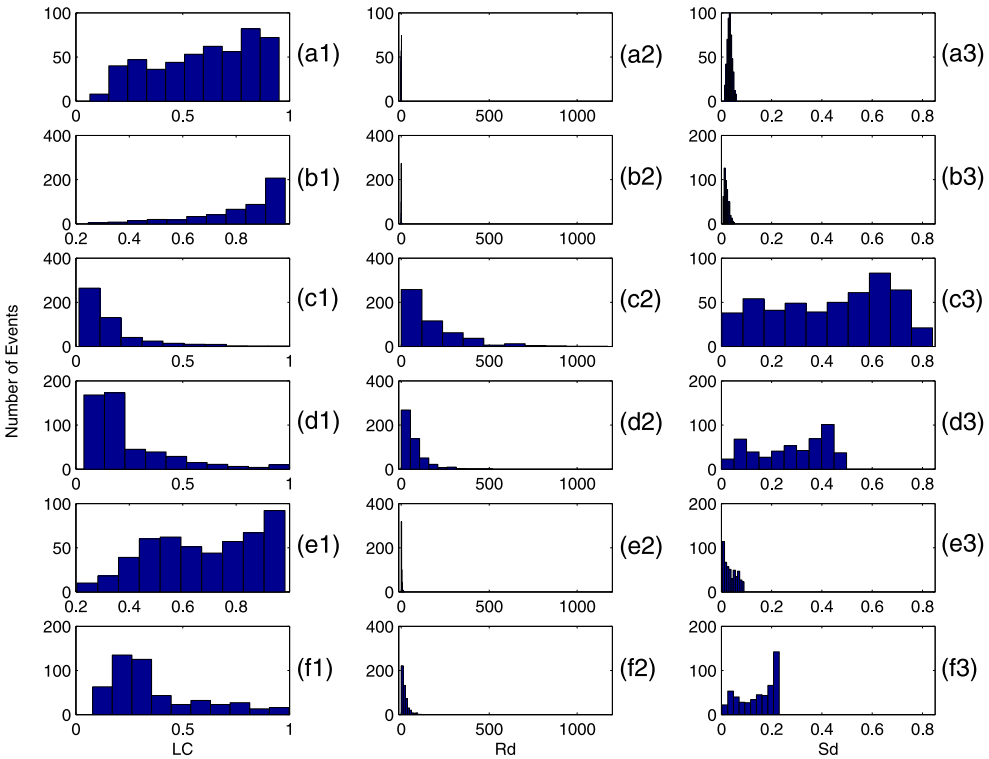


Figure 6. Distributions of the indices *LC*, *Rr*, and *Sd* for the methods for transient in a signal for which the fundamental frequency varies. The following threes from (a1)–(a2)–(a3) to (f1)–(f2)–(f3) show the *LC*, *Rr*, and *Sd* distributions as extracted from SCICA based ($M=3$), SCICA based ($M=5$), CCD, AFW, HPF, and NF methods, respectively.

Copyright © 2015 John Wiley & Sons, Ltd.

DOI: 10.1002/etep

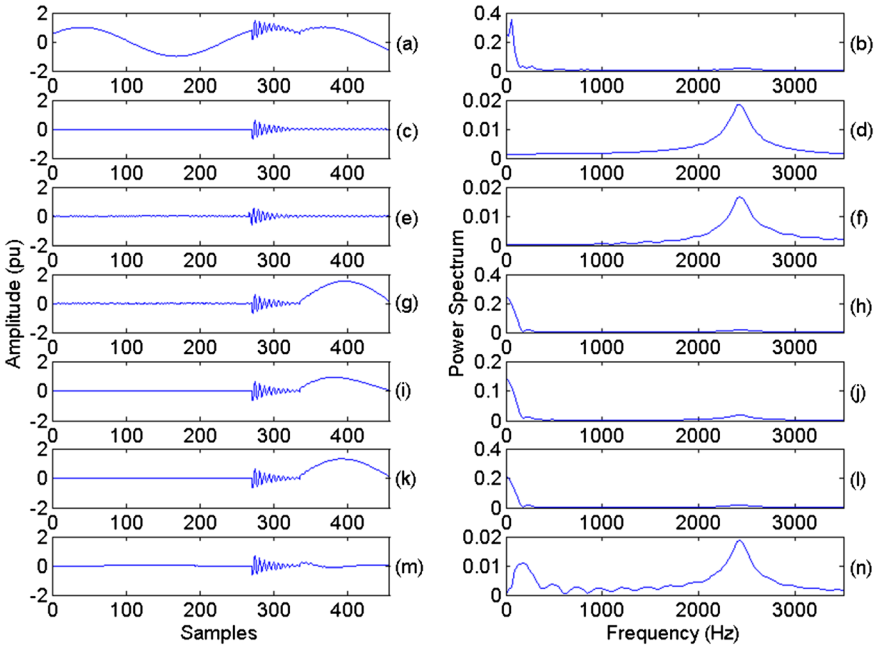


Figure 7. Voltage signal with fundamental frequency varying and corrupted by oscillatory transient in (a) and its spectrum in (b). Original transient source in (c) and its spectrum in (d). The following pairs from (e)–(f) to (m)–(n) show the transient and the respective spectrum as extracted from SCICA based ($M = 5$), AFW, NF, CCD, and HPF methods, respectively.

5.1.5. Voltage signals corrupted by transient and time-varying harmonics. Here, time-varying harmonics have been included at the voltage signals corrupted by transient. The time-varying harmonics were generated by modulating the harmonics (until the seventh component) with abrupt changes of magnitude and phase. From Table V one can see that the proposed method (both cases $M = 3$ and $M = 5$) outperforms the other ones in this case. Among the methods used for comparison, the CCD suffered less from time-varying harmonics.

5.1.6. Synthetic test signal. We have also considered the synthetic test signal created in [1]. This signal consists of a double-frequency transient superimposed on a quasi-steady-state signal (Figure 8). The rms error ε, originally proposed in [1] (Equation (6)), was obtained.

$$\varepsilon = \sqrt{\frac{1}{N_2 - N1}\sum_{N_1}^{N_2}(U_{tr} - U_{xt})^2} \tag{6}$$

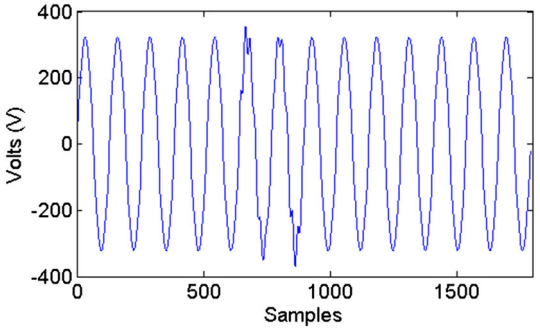


Figure 8. Synthetic test signal reproduced as formulated in [1].

Copyright © 2015 John Wiley & Sons, Ltd.

DOI: 10.1002/etep

with N_1 and N_2 as the starting and ending points of the synthetic transient, and U_{tr} and U_{xt} as the extracted and the original signals, respectively.

Table VI shows the mean value of the error, over 1000 runs. One can see that the proposed method (both cases $M=3$ and $M=5$) achieved the lowest error, in this case.

5.2. *From real data*

In order to verify the efficiency of the proposed method for real signals, the waveforms shown in Figures 9(a), 10(a), and 11(a) were processed by the proposed method ($M=5$) for transient extraction.

The waveform in Figure 9(a) is an experimental current signal corrupted by short and impulsive transients and noise produced at the converter section of a motor starting. The power spectrum of this signal is shown in Figure 9(b). The extracted transient from the proposed method (case $M=5$) is shown in (c) and its power spectrum in (d). One can see that only transient contents have been extracted; that is, low-frequency events have been filtered out by the SCICA-based method. The following pairs from (d)–(e) to (k)–(l) show the transient and its spectrum as extracted from CCD, NF, AFW, and HPF methods, respectively. In Figure 9, the power spectrums were limited to 0.02 in vertical axis and to 5 kHz in horizontal axis to improve visualization aspects and comparison between methods. One can clearly see a strong influence of the fundamental component (60 Hz) at the transient extracted

Table VI. Performance of the methods for the synthetic test signal in terms of the rms error ε.

Methods	ε (V)
Proposed method ($M=3$)	3.35 ± 0.00
Proposed method ($M=5$)	0.87 ± 0.00
Cycle-by-cycle difference	8.00 ± 0.76
Comparison with average fundamental waveform	9.03 ± 0.70
High-pass filter output	5.55 ± 0.13
Notch filter	4.50 ± 0.13

rms, root mean square value.

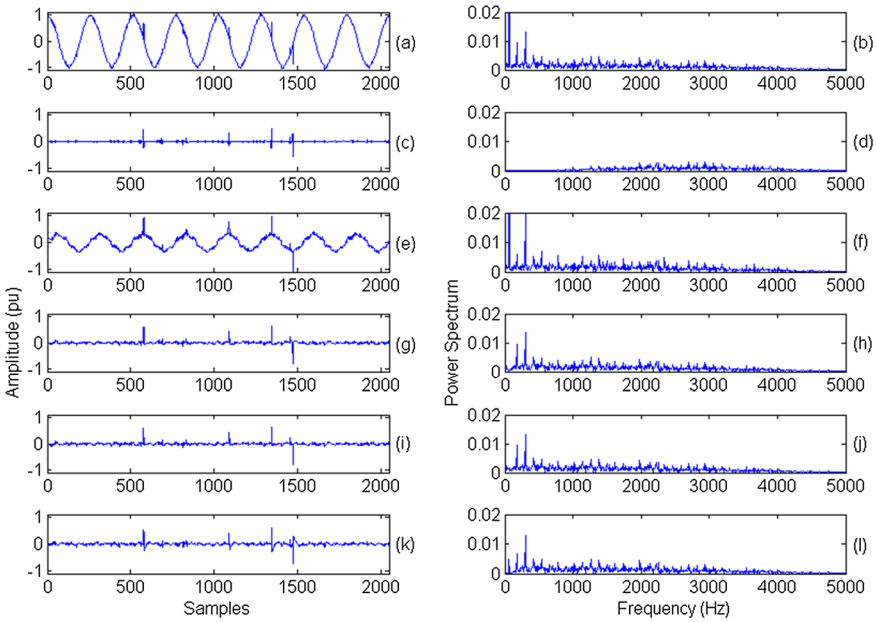


Figure 9. Experimental current signal showing short transients and noise produced at the converter section of a motor starting in (a) and its spectrum in (b). The following pairs from (c)–(d) to (k)–(l) show the transient and its spectrum as extracted from SCICA based ($M=5$), CCD, NF, AFW, and HPF methods, respectively.

Copyright © 2015 John Wiley & Sons, Ltd.

DOI: 10.1002/etep

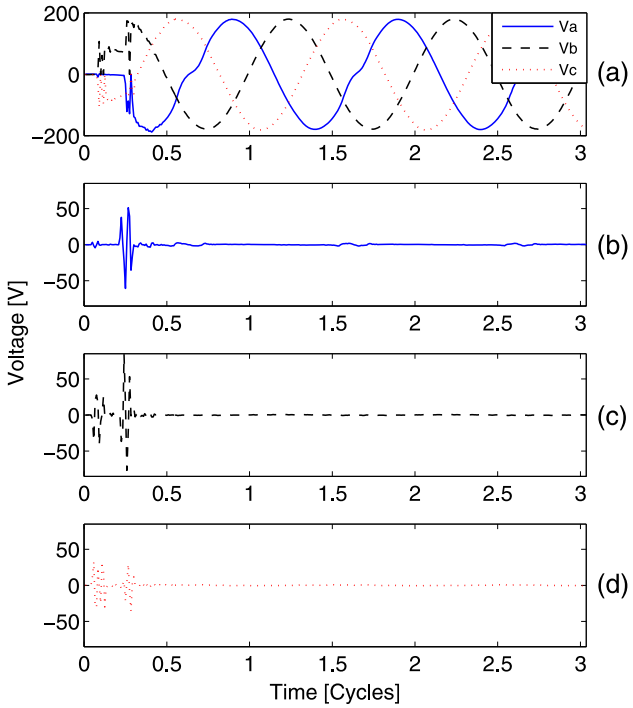


Figure 10. Experimental three-phase voltage signals showing end of interruption with difference in reclosing instants and mild transformer saturation in (a) and the extracted transients by the proposed method ($M = 5$) in (b), (c), and (d), for phases a (Va), b (Vb), and c (Vc), respectively.

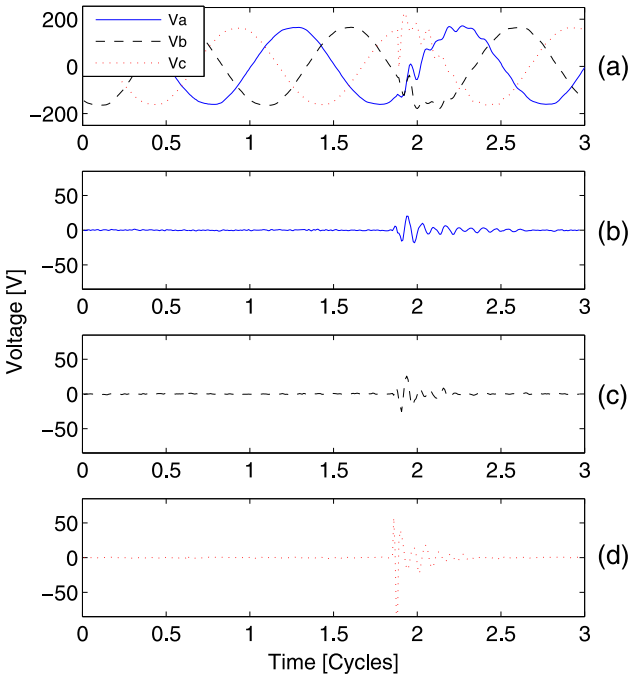


Figure 11. Experimental three-phase voltage signals with voltage transient due to capacitor energizing in (a) and the extracted transients by the proposed method ($M = 5$) in (b), (c), and (d), for phases a (Va), b (Vb), and c (Vc), respectively.

Copyright © 2015 John Wiley & Sons, Ltd.

DOI: 10.1002/etep

by CCD. It is also possible to see harmonics interference at the transients extracted by those methods. The transient extracted by the proposed method (case $M = 3$) was not shown for simplification.

The waveforms in Figure 10(a) are experimental three-phase voltage signals showing end of interruption with difference in reclosing instants and mild transformer saturation. It is observed short transients in the first cycle because of transformer saturation. The transient of each phase extracted by the proposed method ($M = 5$) is shown in (b), (c), and (d), for phases a, b, and c, respectively. It is observed that the method extracted properly the transients of each phase.

The waveforms in Figure 11(a) are experimental three-phase voltage signals with voltage transient due to capacitor energizing. Transients with about half cycle duration can be observed. It is shown the proper transient extraction from the proposed method ($M = 5$) in (b), (c), and (d), for phases a, b, and c, respectively.

6. DISCUSSION

In this section, the pros and cons of each method applied for transient extraction are summarized.

6.1. Cycle-by-cycle difference

According to Sabin *et al*. [28], the CCD method is suitable for capacitor switching transient extraction from the fundamental component. The results in the previous sections show the CCD had poor indices in three of the six simulated cases and achieved the best indices in two of them. The difficulty of this method is associated with the threshold used to compute the transient, because it is dependent on the fundamental frequency deviation.

6.2. Average fundamental waveform

The AFW method overcomes the problem pointed before being well suitable for situation when the fundamental frequency varies. This is because it uses a synthesized sinusoidal component generated by a phase-locked loop synchronized with the fundamental component of the system, so that the difference is performed between the synthesized sinusoidal and the actual signal. The AFW method does not work properly in the presence of harmonics once the phase-locked loop is sensitive to their presence. From the six simulated cases, the AFW method had poor indices in five of them.

Another problem with both methods earlier is regarding sag and swell disturbances that can be detected as transients in the system leading to difficulties in interpretation, especially for statistical results.

6.3. High-pass filter

The HPF method is non-sensitive to frequency variation and works appropriately for high-frequency transients. Another advantage of this method, related with CCD and AFW methods is that sag and swell disturbances are not triggered as transient disturbances. The problem of the HPF method is that high-frequency distortion in the quasi-stationary signal is not removed out by the filter. In this case, threshold setting becomes a challenge and maybe an unsuccessful task, because the parameters adjustment of the HPF will depend on several and particular conditions, some of them of statistical nature. Better than trying to overcome each particular case is looking for a better method for transient detecting and separation, when harmonic distortion is present. The HPF method had poor indices in two of the six simulated cases.

6.4. Notch filter

The NF method is a good way to separate a low-frequency component from high-frequency components (transients). It has been widely used in literature [7,29,30] for PQ disturbance detection and classification and can as well be used to extracting the transient component. Although the algorithm is

Copyright © 2015 John Wiley & Sons, Ltd.

DOI: 10.1002/etep

computationally simple, harmonics will show up in the extracted transient, if the goal is to separate the transient from the fundamental component, because the harmonics are mixed with transient, then the same problem of the HPF method can be pointed out to the NF method. This method had poor indices in two of the six simulated cases.

Summarizing the results achieved with the proposed method in comparison with the others, the proposed method is shown to be the best one in four of the six simulated cases, it was very good in one of them, and it was slightly worse in the first case (Section 5.1.1). Nevertheless, the reached indices in the first case ensure the transients were extracted with an acceptable quality.

7. CONCLUSION

This paper presented a method based on SCICA for efficient extraction of transients from the power system signal. The main advantage of the proposed method is the low influence of harmonics, sags, swells, and rapid voltage changes on the extracted transient waveform and the good performance for slow variations in voltage amplitude, frequency, or distortion. That advantage makes the method general for transient extraction, whereas the traditional methods discussed in this paper have good performance only for specific conditions of the measured voltage or current signal. As can be noted from the results, for the cases where the proposed method was not the best one, it was quite close to the best traditional method.

Additionally, in the operational stage, the proposed method is basically a low-order linear FIR filter. Regarding the two investigated cases ($M=3$ and $M=5$) of the proposed method, the case in which four time-delayed versions ($M=5$) of the monitored signal that are used proved to perform well in all tests.

Furthermore, the proposed method can be applied as a preprocessing tool for transient characterization in disturbance detection, classification, and identification systems. Also, the results may be used for identifying and understanding the causes of transients by correlating the extracted transient with some *a priori* knowledge of the power system.

The efficient extraction of transients may also be useful for calculating PQ indices in transient events. For disturbances with a very different configuration (mainly in terms of frequency range) from those tested in this work, one may redesign the method to achieve the adequate number of time-delayed versions of the monitored signal.

For future works, the authors intend to investigate the use of comb filters in comparison with the methods discussed in this paper.

8. LIST OF SYMBOLS AND ABBREVIATIONS

8.1. Symbols

z	z-transform
H_0	transference function
α_0	notch factor
ρ_0	notch factor
ω_0	system frequency in radians
n	sample index
$x[n]$	time discrete signal
M	dimension of time delayed vector
^{T}	transpose
$y[n]$	estimation of the independent component
$s[n]$	independent component
$\mathbf{W}$	de-mixing matrix
$\mathbf{A}$	mixing matrix
$(i,:)$	row i

Copyright © 2015 John Wiley & Sons, Ltd.

DOI: 10.1002/etep

$\hat{e}[n]$	extracted signal
N	number of samples
η	multiplicative factor
$t[n]$	original transient
$\hat{t}[n]$	extracted transient
Rr	residue ratio
Sd	spectral difference
$S_i(f)$	power spectrum of the original transient
$E_i(f)$	power spectrum of the extracted transient
ε	rms error
N_1	starting point
N_2	ending point
U_{tr}	extracted signal
U_{xt}	original signal

8.2. Abbreviations

PQ	Power quality
SPDs	surge protective devices
HPF	high-pass filter
NF	notch filter
CCD	cycle-by-cycle difference
AFW	average fundamental waveform
ICA	independent component analysis
SCICA	single channel independent component analysis
FIR	finite impulse response
SOBI	second-order blind identification
LC	linear correlation
Rr	residue ratio
Sd	spectral difference
rms	root mean squares

ACKNOWLEDGEMENTS

The authors would like to thank FAPEMIG, CNPq/INERGE, and FAPERJ (Brazil) for supporting this work.

REFERENCES

1. Bollen MHJ, Gu IYH. *Signal Processing of Power Quality Disturbances*, 1st edn. Wiley-Interscience: New York, 2007.
2. IEEE recommended practice for monitoring electric power quality, IEEE Standard 1159–2009.
3. Naik CA, Kundu P. Power quality index based on discrete wavelet transform. *International Journal of Electrical Power & Energy Systems* 2013; **53**:994–1002. DOI:10.1016/j.ijepes.2013.06.024.
4. International Electrotechnical Commission. IEC 61000-4-30: electromagnetic compatibility (EMC)—part 4–30: testing and measurement techniques—power quality measurement methods, Tech. rep., IEC 2008.
5. Shin Y-J, Power EJ, Grady M, Arapostathis A. Power quality indices for transient disturbances. *IEEE Transactions on Power Delivery* 2006; **21**(1):253–261. DOI:10.1109/TPWRD.2005.855444.
6. Liu Z, Zhang Q, Han Z, Chen G. A new classification method for transient power quality combining spectral kurtosis with neural network. *Neurocomputing* 2014; **125**:95–101. DOI:10.1016/j.neucom.2012.09.037.
7. Ribeiro MV, Pereira JLR. Classification of single and multiple disturbances in electric signals. *EURASIP Journal on Advances in Signal Processing* 2007. DOI:10.1155/2007/56918.
8. Radil T, Ramos PM, Janeiro FM, Serra AC. PQ monitoring system for real time detection and classification of disturbances in single phase power system. *IEEE Transactions on Instrumentation and Measurement* 2008; **57**(8):1725–1733. DOI:10.1109/TIM.2008.925345.
9. Santoso S, Maitra A. Empirical estimation of system parallel resonant frequencies using capacitor switching transient data. *IEEE Transactions on Power Delivery* 2005; **20**(2):1151–1156. DOI:10.1109/TPWRD.2005.844280.

Copyright © 2015 John Wiley & Sons, Ltd.

10. Hur K, Santoso S. An improved method to estimate empirical system parallel resonant frequencies using capacitor switching transient data. *IEEE Transactions on Power Delivery* 2006; **21**(3):1751–1753. DOI:10.1109/TPWRD.2006.874559.
11. Santoso S. On determining the relative location of switched capacitor banks. *IEEE Transactions on Power Delivery* 2007; **22**(2):1108–1116. DOI:10.1109/TPWRD.2007.893195.
12. Hur K, Santoso S. Distance estimation of switched capacitor banks in utility distribution feeders. *IEEE Transactions on Power Delivery* 2007; **22**(4):2419–2427. DOI:10.1109/TPWRD.2007.905542.
13. Hur K, Santoso S. On two fundamental signatures for determining the relative location of switched capacitor banks. *IEEE Transactions on Power Delivery* 2008; **23**(2):1105–1112. DOI:10.1109/TPWRD.2008.917669.
14. Ai Y, Zhang H. Harmonic separation based on independent component analysis method. *Journal of Computers* 2013; **8**(2):433–440. DOI:10.4304/jcp.8.2.433-440.
15. He C, Shu Q. Separation and analyzing of harmonics and inter-harmonics based on single channel independent component analysis. *International Transactions on Electrical Energy Systems* 2015; **25**(1):169–179. DOI:10.1002/etep.1832.
16. Ferreira DD, Nagata EA, Ferreira SC, *et al.* Method based on independent component analysis for harmonic extraction from power system signals. *Electric Power Systems Research* 2015; **119**:19–24. DOI:10.1016/j.epsr.2014.09.001.
17. Liu G, Li F, Wen G, Ning S, Zheng S. Classification of power quality disturbances based on independent component analysis and support vector machine, in: International Conference on Wavelet Analysis and Pattern Recognition (ICWAPR), Tianjin, 2013; 115–123. DOI: 10.1109/ICWAPR.2013.6599302.
18. Ferreira DD, de Seixas JM, Cerqueira AS. ICA-based method for power quality disturbance analysis, in: 15th International Conference on Intelligent System Applications to Power Systems, Curitiba, Brazil, 2009; 1–6. DOI: 10.1109/ISAP.2009.5352915.
19. Ferreira DD, de Seixas JM, Cerqueira AS. A method based on independent component analysis for single and multiple power quality disturbance classification. *Electric Power Systems Research* 2015; **119**:425–431. DOI:10.1016/j.epsr.2014.10.028.
20. Davies ME, James CJ. Source separation using single channel ICA. *Signal Processing* 2007; **87**:1819–1832. DOI:10.1016/j.sigpro.2007.01.011.
21. Karimi-Ghartemani M, Iravani M. A nonlinear adaptive filter for online signal analysis in power systems: applications. *IEEE Transactions on Power Delivery* 2002; **17**(2):617–622. DOI: S 0885-8977(02)02727-9.
22. Hirano K, Nishimura S, Mitra SK. Design of digital notch filters. *IEEE Transactions on Communications* 1974; **22**(7):964–970. DOI:10.1109/TCOM.1974.1092311.
23. Hyvärinen A, Karhunen J, Oja E. *Independent Component Analysis*. A Wiley-Interscience Publication: New York, 2001.
24. Belouchrani A, Abed-Meraim K, Cardoso J-F, Moulines E. A blind source separation technique using second-order statistics. *IEEE Transactions on Signal Processing* 1997; **45**(2):434–444. DOI:10.1109/78.554307.
25. Haykin S. *Adaptive Filter Theory*, 4th edn. Prentice-Hall: New Jersey, 2002.
26. Marques CAG, Ferreira DD, Freitas LR, Duque CA, Ribeiro MV. Improved disturbance detection technique for power-quality analysis. *IEEE Transactions on Power Delivery* 2011; **26**(2):1286–1287. DOI:10.1109/TPWRD.2010.2092571.
27. IEEE Industry Applications Society. IEEE guide for the design and application of power electronics in electrical power systems on ships, Tech. rep., IEEE 2008.
28. Sabin DD, Grebe TE, Brooks DL, Sundaram A. Rules-based algorithm for detecting transient overvoltages due to capacitor switching and statistical analysis of capacitor switching in distribution systems, in: IEEE Transmission and Distribution Conference, Vol. 2, New Orleans, LA, 1999; 630–635 vol. 2. DOI: 10.1109/TDC.1999.756124.
29. Ribeiro MV, Marques CAG, Cerqueira AS, Duque CA, Pereira JLR. Detection of disturbances in voltage signals for power quality analysis using HOS. *EURASIP Journal on Advances in Signal Processing* 2007; **2007**:13–25. DOI:10.1155/2007/59786.
30. Barbosa BHG, Ferreira DD. Classification of multiple and single power quality disturbances using a decision tree-based approach. *Journal of Control, Automation and Electrical Systems* 2013; **24**(5):638–648. DOI:10.1007/s40313-013-0061-y.

Copyright © 2015 John Wiley & Sons, Ltd.